Journal of Non-Crystalline Solids 629 (2024) 122874

Contents lists available at ScienceDirect

Journal of Non-Crystalline Solids

journal homepage: www.elsevier.com/locate/jnoncrysol

Physical aging of a biodegradable alicyclic polymer: poly (pentamethylene *trans*-1,4-cyclohexanedicarboxylate)

Marouane Mejres [a], Kylian Hallavant [a], Giulia Guidotti [b], Michelina Soccio [b,c,d], Nadia Lotti [b,c,e], Antonella Esposito [a], Allisson Saiter-Fourcin [a,*]

[a] Univ Rouen Normandie, INSA Rouen Normandie, CNRS, Groupe de Physique des Matériaux UMR 6634, F-76000 Rouen, France
[b] Department of Civil, Chemical, Environmental and Materials Engineering, University of Bologna, Via Terracini 28, 40131 Bologna, Italy
[c] Interdepartmental Center for Industrial Research on Advanced Applications in Mechanical Engineering and Materials Technology, CIRI-MAM, Viale del Risorgimento 2, 40136, Bologna, Italy
[d] Interdepartmental Center for Industrial Research on Buildings and Construction CIRI-EC, Via del Lazzaretto 15/5, 40131, Bologna, Italy
[e] Interdepartmental Center for Agro-Food Research, CIRI-AGRO, Via Quinto Bucci 336, 47521, Cesena, Italy

ARTICLE INFO

Keywords:
Enthalpy of recovery
Relaxation processes
FSC
DSC
Polyesters

ABSTRACT

Physical aging of poly (pentamethylene *trans*-1,4-cyclohexanedicarboxylate) (PPeCE), a biodegradable alicyclic polyester, was investigated using Fast Scanning Calorimetry (FSC), a recent calorimetric technique allowing to accelerate physical aging and study the associated relaxation processes at different aging temperatures in an experimentally-reasonable time scale. Different mechanisms were highlighted by varying the aging temperature on a temperature range of more than 60 °C. At aging temperatures well below the glass transition temperature, several relaxation mechanisms were evidenced, probably related to secondary relaxation processes (β relaxations). When the aging temperature approaches the glass transition temperature, the primary relaxation process (α relaxation) becomes predominant.

1. Introduction

Many studies have recently focused on developing biobased and/or biodegradable plastics that could be competitive with traditional plastics. Ideally, these materials would be made from renewable resources and, at their end-of-life, provided specific conditions, they would degrade into carbon dioxide and/or methane, water, and other substances harmless to their degradation environment. Traditionally, the development of biodegradable polymers has been limited to linear aliphatic polyesters, such as polyglycolide (PGA), polylactides (PLAs), polycaprolactone (PCL) or polyhydroxyalkanoates (PHAs). Indeed, aliphatic polyesters have a very strong aptitude to biodegrade, mostly due to the potential of ester groups to undergo hydrolytic chain scissions; their performance, though, is generally poor compared to petroleum-based aromatic polymers [1]. Poly (alkylene 1,4-cyclohexanedicarboxylate)s (PCHs) are alicyclic polyesters with an in-chain aliphatic ring and a variable number of methylene groups, depending on the diol selected to react with 1,4-cyclohexanedicarboxylic acid (CHDA). *trans*-1,4-CHDA may be either petroleum-based or derived from renewable sources, specifically from succinic acid [2–8] and biobased terephthalic acid, which is in turn sourced from limonene [9]. PLAs can be counted amongst the first biobased and biodegradable polyesters that were developed and scaled up from laboratory to industrial scale, eventually finding some applications in the packaging domain; however, PLAs have relatively poor mechanical and barrier properties, which forces the industrials to either modify or incorporate them into complex formulations [10–14]. Polyesters containing alicyclic units, such as PCHs, offer several benefits in terms of tensile strength, stiffness, impact resistance and thermal stability, along with the advantage of being potentially degradable [15]. These features make them particularly suitable for packaging [16–18] and biomedical [19,20] applications. Irrespective of the application expected for these polyesters, understanding and predicting their behavior over time is crucial and requires the investigation of physical aging, because any rearrangement of the macromolecular chains in the amorphous phase over time has the potential of significantly affect not only the relaxation dynamics [21], but also the macroscopic behavior, including barrier, adhesion and mechanical properties [22–28].

Physical aging is a natural phenomenon implying the molecular mobility in the amorphous phase, and modifying its density. As

* Corresponding author.
E-mail address: allison.saiter@univ-rouen.fr (A. Saiter-Fourcin).

https://doi.org/10.1016/j.jnoncrysol.2024.122874
Received 20 December 2023; Received in revised form 9 February 2024; Accepted 12 February 2024
Available online 21 February 2024
0022-3093/© 2024 The Author(s). Published by Elsevier B.V. This is an open access article under the CC BY-NC-ND license (http://creativecommons.org/licenses/by-nc-nd/4.0/).

highlighted by Kovacs [29], this phenomenon is nonlinear and non-exponential, depending on the time and temperature at which it occurs. Whatever the nature of the material (thermoplastic polymers [30–32], thermosets [33], chalcogenide glasses [34,35], pharmaceutical compounds [36], etc.), and whether it is fully amorphous or semi-crystalline with a residual amorphous phase, the latter will undergo physical aging anytime the material is maintained at an aging temperature (T_{ag}) below its glass transition temperature (T_g) [37]. Physical aging is associated with a so-called enthalpy of recovery, an endothermic peak superimposed to the specific heat capacity step at the glass transition during a heating ramp recorded on an aged sample. As such, physical aging can be investigated through calorimetric measurements, and its quantification is directly related to the area of this endothermic peak superimposed to the specific heat capacity step at T_g [38,39]. However, physical aging is also a self-slowing phenomenon; for this reason, it is sometimes impossible to fully investigate it at the laboratory time-scale, enforcing researchers to make predictions based on models [40–43] that are not always reliable, especially to predict the consequences of long-term aging [44]. In recent years, the development of Fast Scanning Calorimetry (FSC) has provided a possibility to experimentally investigate physical aging in acceptable times on its entire time-scale, which represents a major step forward with respect to classical DSC analysis [45–47]. Indeed, FSC allows cooling down a glass-forming liquid at extremely high rates (from 0.1 K/s up to 40 000 K/s), vitrifying it at high glass transition temperatures, i.e. with more free volume and higher molecular mobility, which in turn accelerates physical aging.

When the cooling rate is too high for a glass-forming liquid to maintain an equilibrium state, the obtained glass is intrinsically out-of-equilibrium, i.e. its specific volume, enthalpy, and entropy are higher than they would have been in the corresponding equilibrium state (liquid-like state extrapolated to low temperatures). This thermodynamic excess initiates a progressive relaxation process towards equilibrium. Calorimetric analysis can be used to monitor the enthalpy of recovery associated with physical aging for a given time (t_{ag}) in isothermal conditions (T_{ag}) by integrating the enthalpy difference between the scans recorded on an aged and successively rejuvenated sample, according to Eq. (1):

$$\Delta H\left(T_{ag}, t_{ag}\right) = \int_{T_1}^{T_2} \left[c_{p,a}(T) - c_{p,r}(T)\right] dT \quad (1)$$

Where $c_{p,a}$ (T) and $c_{p,r}$ (T) are the specific heat capacities of the aged and rejuvenated sample respectively, and T_1 and T_2 are arbitrary temperatures below and above the glass transition temperature T_g. Under the assumption that the thermodynamic equilibrium is reached for an infinite aging time, the expected enthalpy of recovery (ΔH_∞) can be estimated according to Eq. (2):

$$\Delta H_\infty = \Delta c_{p,\left(T_{g\ mid}\right)} \cdot \left(T_{g\ mid} - T_{ag}\right) \quad (2)$$

Where T_{ag} corresponds to the aging temperature, $T_{g\ mid}$ is the glass transition temperature taken at half-height of the glass transition step, and $\Delta c_{p,(Tg\ mid)}$ is the step in specific heat capacity extrapolated at $T_{g\ mid}$.

One way for checking if a glass has reached its equilibrium state, is to compare the experimental enthalpy of recovery calculated from Eq. (1) after a given t_{ag} at a given T_{ag}, to the theoretical value estimated from Eq. (2) at the same aging temperature.

However, it is still unclear how a glass reaches its equilibrium state after an extended time of physical aging. In 1995, J.L. Gomez Ribelles et al. [43] believed that polymeric glasses could never reach the thermodynamic equilibrium due to their large steric constraints. In 2013, D. Cangialosi et al. [48] suggested that the thermodynamic equilibrium could still be achieved, but with the emergence of a variable number of intermediate states, whose number depends on the gap between T_g and T_{ag}. This hypothesis has been confirmed in recent studies on different materials [49,50]. In 2018, R. Androsch et al. [51] added that not only the thermodynamic equilibrium is achievable, but it is also possible to eventually reach the crystalline state; this hypothesis has been successively confirmed in the case of chalcogenide glasses [52]. In 2000, J.M. Hutchinson et al. [42] suggested that only a fraction of a glass-forming liquid is actually vitrified during the glass transition. As a consequence, the theoretical thermodynamic equilibrium would never be reached as expected due to the coexistence of two types of relaxation processes, i.e. a slow one for the vitrified polymer fraction, and a fast one for the non-vitrified polymer fraction. In 2022, Z. Song et al. [53] evidenced fast equilibration mechanisms in the amorphous phase of polymers related to slow liquid dynamics, called Slow Arrhenius Process (SAP).

The aim of this work is to investigate the physical aging of an alicyclic polyester out of the PCHs family, i.e. poly (pentamethylene *trans*-1,4–cyclohexanedicarboxylate) (PPeCE), which has been anticipated as a good candidate to replace petroleum-based polymers, having interesting biodegradability properties yet acceptable performances. To this purpose, classical DSC and FSC measurements have been performed at different aging temperatures and durations. The kinetics of the observed aging processes were discussed according to the different models proposed in the literature.

2. Experimental section

2.1. Synthesis

The synthesis of poly (pentamethylene *trans*-1,4–cyclohexanedicarboxylate) (PPeCE) was carried out in bulk by a two-step melt polycondensation procedure, starting from *trans*-1,4–cyclohexanedicarboxylic acid, 1,5-pentanediol (in a 100% molar excess) and titanium tetrabutoxide (TBT, 200 ppm) as catalyst, within a stirred 250-mL glass reactor in a thermostated bath. The large molar excess of diol with respect to the diacid promoted the dissolution of the latter. In brief, during the first stage, which was carried out at 1 atm under pure nitrogen flow, the temperature was set to 190 °C and kept constant for about 1.5 h after the complete dissolution of the diacid. During this time, about 90% of the theoretical amount of water was distilled off. At the beginning of the second stage, the temperature was raised to 210 °C and pressure was gradually reduced until 0.06 mbar to promote the transesterification reactions and the removal of the glycolic excess. The synthesis was carried out for 2 additional hours, until a high and constant torque value was measured, indicating that a high molecular weight was reached. After the synthesis, the polymer was purified by dissolving it in chloroform and precipitating it in a beaker filled with methanol in large excess (chloroform:methanol / 1:10). After purification by dissolution in chloroform and precipitation in methanol, the sample was dried under vacuum (1 h at 0.1 mbar).

2.2. Molecular characterization

^{1}H NMR analysis was carried out to confirm the chemical structure of PPeCE given in Fig.1. The spectrum was acquired using a Varian XL-400 NMR spectrometer (Palo Alto, CA, USA) at room temperature (relaxation time = 0 s, acquisition time = 1 s, 100 repetitions). The polymer was dissolved by introducing about 15 mg of sample in 1 mL of deuterated chloroform (containing 0.03% tetramethylsilane, TMS, as internal reference).

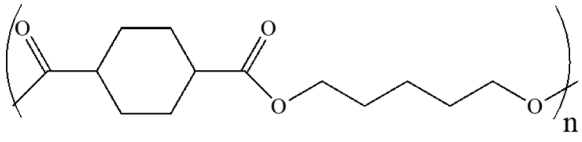

Fig. 1. Chemical structure of poly (pentamethylene *trans*-1,4-cyclohexanedicarboxylate).

The number average molecular weight ($\overline{M_n}$) and the dispersity ($Đ$) were estimated by Gel Permeation Chromatography (GPC) analysis performed at 30 °C using an HPLC 1100 chromatograph (Agilent Technologies, Santa Clara, CA, USA) equipped with a PLgel 5 mm MiniMIX-C column. A chloroform solution was used as eluent with a flow of 0.3 mL/min, and sample concentrations of about 2 mg/mL were adopted. The calibration curve was obtained using polystyrene standards with a molecular range of 800–100 000 g/mol.

2.3. Thermal characterization

Before any thermal characterization, the material was stored under vacuum in a desiccator in the presence of P_2O_5 to reduce the exposure to humidity. Preliminary characterizations of the glass transition temperature domain were conducted by Differential Scanning Calorimetry (DSC), using a DSC 3+ (Mettler Toledo) equipped with an FRS6 sensor, and with the support of the STARe software for data analysis. Calibrations for temperature, enthalpy, and tau lag were achieved using zinc, indium, and water standards. A sample of PPeCE with a mass of 1.86 mg was placed in a 40 µl sealed aluminum pan and a continuous nitrogen gas flow of 50 mL/min was maintained in the cell. The measurements consisted in rejuvenating the sample by heating it up above the melt (110 °C), then cooling it down to −80 °C at a rate of 30 K/min, identified as the slowest cooling rate to achieve amorphization. Subsequently, a heating scan at a rate of 10 K/min was performed to obtain the curve corresponding to the rejuvenated sample (Fig. S1). This curve provided the specific heat capacity step at the glass transition temperature (Δc_p), which is necessary for estimating the sample mass in FSC measurements.

Fast Scanning Calorimetry (FSC) experiments were performed with a Flash DSC2+ (Mettler Toledo) equipped with a Huber TC100 intra cooler, which allows to cool the sample down to −95 °C at extremely high cooling rates. Few nanograms (51 ± 5 ng) of PPeCE were placed on a MultiSTAR UFH chip sensor with the help of a microscope. The FSC measurements were all performed on the same sample. The FSC chamber was continuously flushed by 50 mL/min nitrogen gas flow to avoid water condensation [54]. FSC calibration consisted in conditioning the chip sensor and making the necessary corrections for temperature lags (as detailed in the Results and discussion section). The heating and cooling scanning rates were fixed at $\beta_h = |\beta_c| = 1500$ K/s. These conditions prevented both the crystallization from the melt (during cooling) and the subsequent cold crystallization (during heating), ensuring that the sample always remains amorphous. As proposed in the literature [55], the sample mass was estimated by comparing the heat flow step measured by FSC (at $\beta_h = |\beta_c| = 1500$ K/s) with the specific heat capacity step measured by DSC (at $\beta_h = |\beta_c| = 10$ K/min), under the assumption that the specific heat capacity step is the same for both techniques. Physical aging was then investigated by performing the thermal protocol illustrated in Fig. 2:

The first heating-cooling-heating cycle between −95 °C and 110 °C was performed to erase any possible thermal history of the sample and ensure a good contact between the sample and the membrane of the chip sensor. Then, the system was cooled down from the melt to the selected aging temperature (T_{ag}) and kept in isothermal conditions during the selected aging time (t_{ag}). After aging, the system was cooled down again to −95 °C for the final heating ramp. Finally, another cooling-heating cycle was applied to record the response of the rejuvenated sample to be compared with the response of the aged sample.

3. Results and discussion

The spectrum obtained by ^{1}H NMR (Fig. S2) confirms the chemical structure of a PPeCE homopolyester, as illustrated in Fig. 1. Besides the signals due to the solvent and to TMS, one can clearly detect the peaks related to the cyclohexane moiety, i.e. a *trans* (2.25 ppm), a *cis* (2.41 ppm), and b (2.00 and 1.42 ppm), as well as the signals referring to the pentamethylene subunit, i.e. c (4.11 ppm), d (1.63 ppm), and e (1.42 ppm). The percentage of *cis*-isomer in the 1,4-cyclohexanedicarboxylate subunit was calculated from the ratio of the areas under the a *cis* and a *trans* signals, and found to be of 5.4% . A careful control over the aforementioned synthesis procedure ensured a good distribution of the molecular weights, with a high value of $\overline{M_n}$ (57 855 g/mol) and a narrow value of dispersity ($Đ = 1.4$).

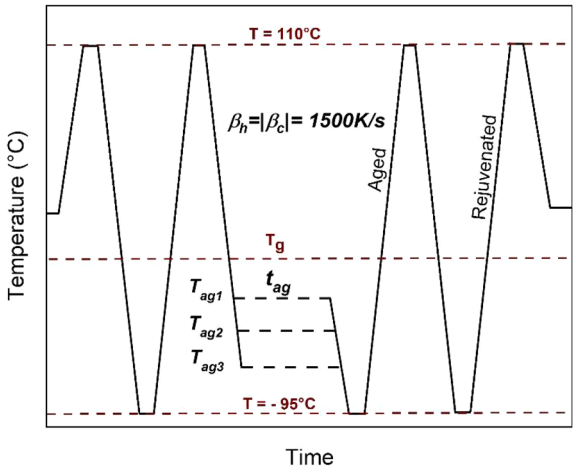

Fig. 2. Experimental protocol for physical aging experiments on PPeCE. The aging temperatures are $T_{ag1} = -15$ °C, $T_{ag2} = -20$ °C, $T_{ag3} = -30$ °C, the aging time is $t_{ag} = 10$ min, and T_g corresponds to the glass transition temperature estimated from FSC curves, i.e. $T_g = 3$ °C. The scanning rates are $\beta_h = |\beta_c| = 1500$ K/s.

Fig. 3a shows the normalized heat flow recorded during the heating and cooling ramps with a scanning rate of 1500 K/s. As expected, the glass transition is shifted to higher temperatures in comparison to the value obtained by classical DSC (Fig. S1). Indeed, the higher the cooling rate used to form a glass, the higher its glass transition temperature. By comparing the heating and cooling scans, one may note that T_g on cooling is slightly shifted to lower temperatures compared to T_g on heating. This shift can be attributed to the dynamic thermal lag due to the large scanning rates, which makes it necessary to apply a correction for the estimation of the glass transition temperature prior to perform the aging protocols [55]. Fig. 3b shows the fictive temperatures estimated both on cooling ($T_{f,c}$) and on heating ($T_{f,h}$) using the method proposed by Moynihan et al. [56]. The difference between $T_{f,h} = 2.5°C$ and $T_{f,c} = 0.6°C$ is used to calculate the dynamic correction factor $\Delta T_D = \frac{T_{f,h} - T_{f,c}}{2}$ [55]. In this case, ΔT_D is about 1 °C; such a small value of dynamic thermal lag confirms that the sample thickness and shape are optimal, ensuring an efficient thermal transfer. The corrected value of T_g is then estimated by adding ΔT_D to the value of $T_{g\ mid\ (Cooling)}$ calculated from the cooling ramp, i.e. $T_g = 2$ °C + $\Delta T_D = 3$ °C. This value was chosen as the reference glass transition temperature for all the subsequent physical aging thermal protocols. Thus, concerning the calculation of the infinite enthalpy of recovery (Eq. (2)), the value taken for $T_{g\ mid}$ is 3 °C.

To evaluate the influence of temperature on the relaxation behavior occurring during the physical aging processes, isochronal measurements were first carried out with a fixed time of 10 min at different aging temperatures going from −60 °C up to 10 °C. The results are reported in Fig. 4a.

Irrespective of the aging temperature, the value of the specific heat capacity step at the glass transition Δc_p is constant, proving that the amount of amorphous phase implied in the aging process is constant, and that there is no mass loss and no degradation during the cycling. This proves that only physical aging occurs and the process is totally reversible as expected. When T_{ag} is far from the glass transition, more

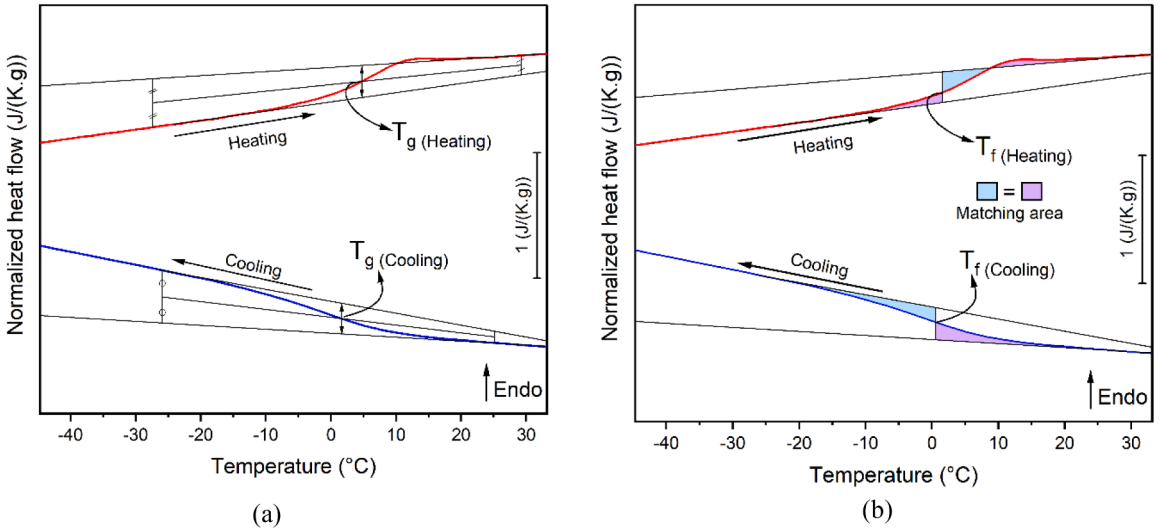

Fig. 3. Normalized heat flow recorded for PPeCE on heating and cooling with scanning rates $\beta_h = |\beta_c| = 1500$ K/s. (a) Method used to determine the mid-point glass transition temperature $T_{g\ mid}$ from the cooling and heating ramps. (b) Estimation of the fictive temperature T_f from the cooling and heating ramps according to the method of the matching areas [56].

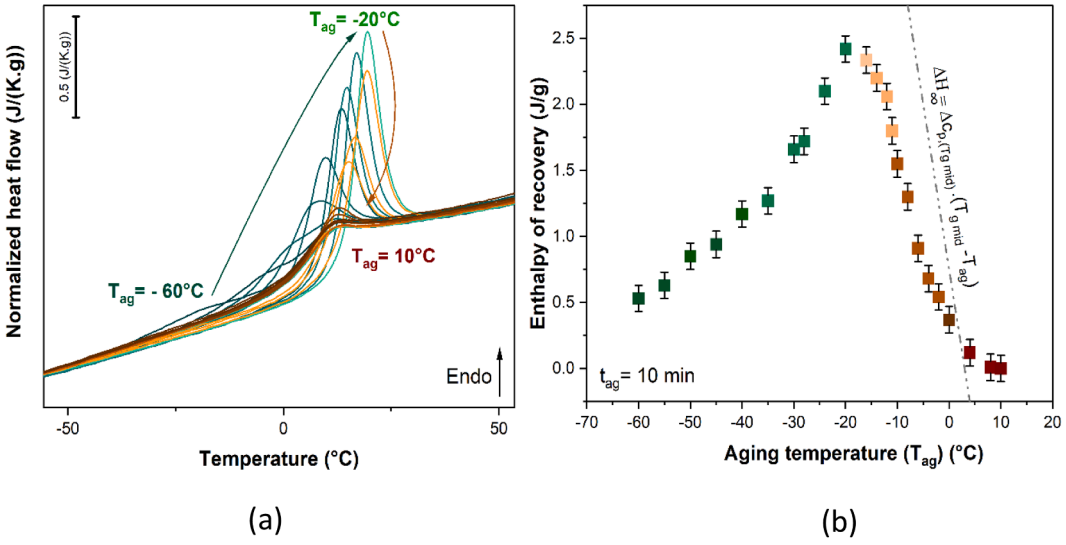

Fig. 4. (a) FSC curves for PPeCE aged during 10 min at different aging temperatures (from −60 °C up to 10 °C). (b) Enthalpy of recovery estimated from Fig. 4(a) and Eq. (1) for each aging temperature. Error bars of 0.2 J/g were added based on the measurement uncertainty for area calculations in the OriginPro software. The dotted line corresponds to the evolution of $\Delta H\infty$ as a function of T_{ag}.

precisely at −50 °C and −60 °C, an endothermic overshoot appears before the specific heat capacity step at the glass transition. This unexpected signature has been recently discussed by X. Monnier et al. [49]. They confirmed that this endothermic peak is a real feature of the physical aging process. Thus, this behavior supports the hypothesis that other mechanisms are involved during the aging processes, whose signature is well visible at temperatures far below the glass transition temperature, and could correspond to secondary relaxation processes related to motions at a smaller scale than the repeating unit [57]. When T_{ag} is increased from −60 °C up to −20 °C, an expected increase of the endothermic peak area superimposed to the specific heat capacity step at the glass transition is observed, along with an expected shift of this peak towards higher temperatures. When T_{ag} is further increased from −20 °C up to 10 °C (i.e. until entering the glass transition temperature range), the opposite behavior is observed, with a decrease of the endothermic peak area and its shift back to lower temperatures. Fig. 4b shows the evolution of the enthalpy of recovery estimated from Eq. (1) for each aging temperature when the sample is aged during 10 min. These results evidence two different behaviours highlighted by cold and hot color palettes, respectively. Furthermore, the enthalpy of recovery drops to zero when the glass transition temperature is reached, i.e. for $T_{ag} \geq 3$ °C. This bell-shaped behavior has been already shown in the literature [58–60] and explained by considering two different contributions to the physical aging process, i.e. one kinetic and one thermodynamic. For a given aging time t_{ag} at temperatures far from the glass transition temperature, the molecular mobility and consequently the rate of densification are very low, resulting in small values of the enthalpy of recovery, which means that physical aging is mainly kinetically controlled. If aging time is kept constant and the aging temperature is slightly increased, the molecular mobility is facilitated and therefore the enthalpy of recovery increases. As the aging temperature further approaches the glass transition temperature, the difference between ΔH_∞ and $\Delta H(T_{ag}, t_{ag})$ further decreases; the aging process is then thermodynamically controlled, and any increase in T_{ag} implies a decrease in ΔH_∞

and $\Delta H(T_{ag}, t_{ag})$. The maximum of the bell-shaped behavior is observed when the aging process turns from mainly kinetically to thermodynamically controlled.

After evaluating the influence of the aging temperature for a given aging time, the same sample was aged at selected aging temperatures (−15 °C, −20 °C and −30 °C) during different aging times (from 0.1 s up to 20,000 s). The results are reported in Fig. 5.

T_{ag} = −20 °C has been chosen because it corresponds to the temperature at which the aging process starts to be thermodynamically controlled (Fig. 4(b)); two additional temperatures have been selected to investigate physical aging process mostly dominated by either kinetics (T_{ag} = −30 °C) or thermodynamics (T_{ag} = −15 °C).

Fig. 5 shows that PPeCE's physical aging follows the expected trend irrespective of the selected aging temperature, i.e. with an increasing aging time, the endothermic peak superimposed to the specific heat capacity step at the glass transition becomes more pronounced and gets shifted towards higher temperatures. Furthermore, irrespective of the aging temperature and of the aging time, the value of the specific heat capacity step at the glass transition Δc_p is constant, proving that the amount of amorphous phase implied in the aging process is constant, confirming that there is no mass loss and no degradation during the cycling.

For each aging temperature and each aging time, the enthalpy of recovery ΔH_{tag} was calculated according to Eq. (1). The difference between the infinite enthalpy of recovery ΔH_∞ (maximum enthalpy of recovery expected at an infinite aging time) and ΔH_{tag} is then calculated and plotted as a function of the aging time (Fig. 6). As expected, and whatever the aging temperature, the longer the aging time, the smaller the difference between ΔH_∞ and ΔH_{tag}, proving that the sample tries to reach its equilibrium state, but unsuccessfully for aging times as long as 20,000 s since zero is not reached. This means that the physical aging process needs longer times to be fully achieved. Interestingly, a stepwise decrease is observed, as highlighted by the gray dotted lines traced between 10 and 500 s in Fig. 6. Even more interestingly, the slope of these lines is the same, irrespective of the aging temperature T_{ag}, suggesting that the rate of physical aging at the considered aging temperatures in this range of aging times is identical. One may wonder how the chemical composition and structure affect physical aging; for this reason, the results obtained for PPeCE were compared to the ones previously obtained for poly (lactic acid) (PLA) in equivalent conditions, i.e. when aging is performed 18 °C below the glass transition temperature during 20,000 s [47]. It appears that physical aging has similar kinetics in both systems, irrespective of their chemical composition and structure, because (ΔH_∞ - ΔH_{tag}) = 2 J/g for PLA [47] and 1.5 J/g for PPeCE.

By selecting different aging temperatures T_{ag}, the presence of intermediate plateaus is clearly evidenced (Fig. 6), revealing the existence of multi-time scales for glass equilibration. As recently proposed by Cangialosi et al. [48,49], this could be attributed to additional relaxation modes supporting the main structural relaxation, which are faster and less cooperative because associated with local molecular motions. This

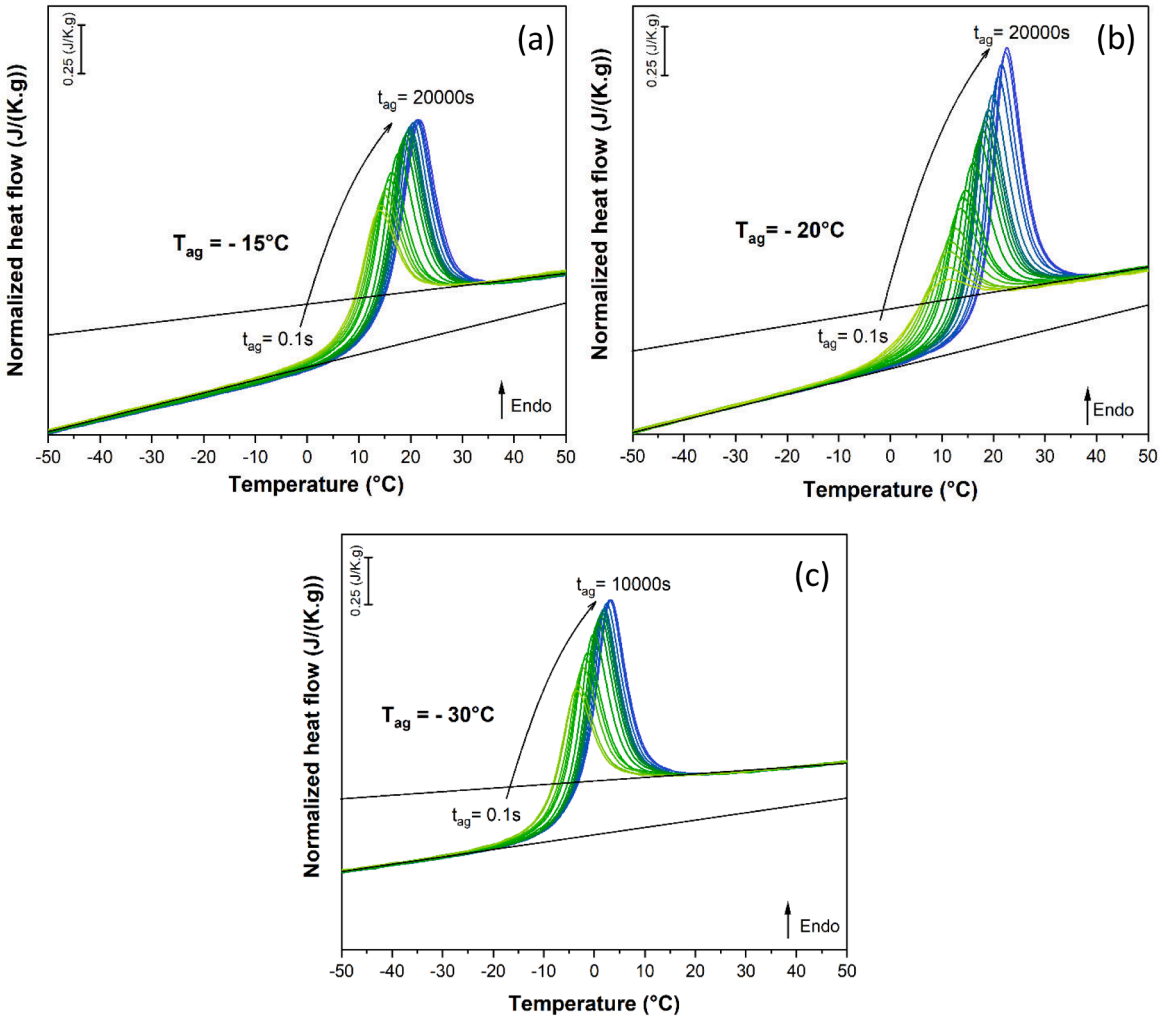

Fig. 5. FSC curves for PPeCE after different aging times (from 0,1 s up to 20000s) at three aging temperatures, i.e. (a) T_{ag} = −15 °C, (b) T_{ag} = −20 °C, and (c) T_{ag} = −30 °C.

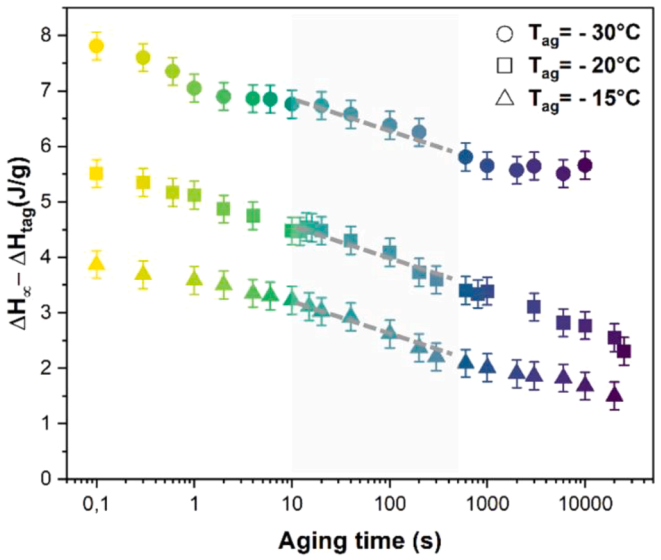

Fig. 6. Evolution of the difference between the infinite enthalpy of recovery ΔH_∞ (maximum enthalpy of recovery expected at an infinite aging time) and the actual enthalpy of recovery ΔH_{tag} for PPeCE aged at three temperatures: T_{ag} = −30 °C (circles), T_{ag} = –20 °C (squares), and T_{ag} = −15 °C (triangles). The aging times range between 0.1 s and 20,000 s. Error bars of 0.2 J/g were added based on the measurement uncertainty for area calculations in the OriginPro software. The gray dotted lines are guides for the eye.

observation agrees with the fact that dielectric relaxation spectroscopy previously evidenced the presence of two secondary relaxation processes (β_1 and β_2) in poly (trimethylene *trans*-1,4-cyclohexanedicarboxylate) (PPCE) [61], which also belongs to the PCHs family and differs from PPeCE only in terms of number of methylene groups (3 in PPCE, 5 in PPeCE). In PPCE, these two distinct contributions have been attributed to changes in the conformation of the flexible bonds within the repeating unit, eventually leading to intramolecular movements. In particular, the high-frequency mode (β_1) has been related to the rotation of the ester oxygen bound to the aliphatic carbon in the diol subunit, whereas the low-frequency mode (β_2) would be related to the chemical bond between the aliphatic ring carbon and the ester carbon. It is reasonable to assume that the secondary relaxation modes observed in PPCE also occur in PPeCE, given the similarity of their repeating units. Considering all the evidences, and the discussions previously reported in the literature about similar cases, it seems likely to attribute the plateaus in Fig. 6 to the support brought by local secondary relaxation modes to the main relaxation process, that is still dominating the process of physical aging [49].

4. Conclusion

Physical aging of a potentially biobased and biodegradable alicyclic polyester, poly (pentamethylene *trans*-1,4-cyclohexanedicarboxylate) (PPeCE), was investigated by calorimetric analyses (DSC and FSC). Thanks to the extremely fast heating and cooling scanning rates provided by FSC, the relaxation processes involved in physical aging have been evidenced for a specific aging time at different aging temperatures. At aging temperatures far below the glass transition temperature, several mechanisms have been observed, likely linked to secondary relaxation processes (β relaxations). When the aging process is performed at a temperature close to the glass transition temperature, the main relaxation process (α relaxation) becomes predominant. Despite the differences in chemical composition and configuration of the repeating unit, the kinetics of physical aging observed for PPeCE appear to be equivalent to the one observed for PLA in equivalent aging conditions, i.e. equivalent aging time and equivalent gap between T_g and T_{ag}. PLA is one of the most investigated and currently developed biobased and biodegradable polyester, and this suggests that PPeCE could be a potential concurrent of PLA for packaging, especially in the case of frozen food.

CRediT authorship contribution statement

Marouane Mejres: Writing – original draft, Methodology, Investigation, Formal analysis, Data curation. **Kylian Hallavant:** Writing – review & editing, Methodology, Investigation, Formal analysis, Data curation. **Giulia Guidotti:** Writing – review & editing, Investigation, Funding acquisition, Formal analysis, Data curation. **Michelina Soccio:** Writing – review & editing, Investigation, Funding acquisition, Formal analysis, Data curation. **Nadia Lotti:** Funding acquisition. **Antonella Esposito:** Writing – review & editing, Supervision, Project administration, Funding acquisition. **Allisson Saiter-Fourcin:** Writing – review & editing, Writing – original draft, Validation, Supervision, Resources, Project administration, Methodology, Funding acquisition, Conceptualization.

Declaration of competing interest

The authors declare that they have no known competing financial interests or personal relationships that could have appeared to influence the work reported in this paper.

Data availability

Data will be made available on request.

Acknowledgements

The authors acknowledge the financial support provided by the Normandy Region through the Graduate School Materials & Energy Sciences (GS-MES) and the Laboratory of Excellence Energy, Materials & Clean Combustion Center (LabEx EMC3). Furthermore, the authors acknowledge Mettler Toledo for lending the DSC 3+.

Supplementary materials

Supplementary material associated with this article can be found, in the online version, at doi:10.1016/j.jnoncrysol.2024.122874.

References

[1] A. Larrañaga, E. Lizundia, A review on the thermomechanical properties and biodegradation behaviour of polyesters, Eur. Polym. J. 121 (2019) 109296, https://doi.org/10.1016/j.eurpolymj.2019.109296.
[2] B. Vanhaecht, M.N. Teerenstra, D.R. Suwier, R. Willem, M. Biesemans, C.E. Koning, Controlled stereochemistry of polyamides derived from *cis/trans*-1,4-cyclohexanedicarboxylic acid, J. Polym. Sci. Part Polym. Chem. 39 (2001) 833–840, https://doi.org/10.1002/1099-0518(20010315)39:6<833::AID−POLA1056>3.0.CO;2-5.
[3] D.J. Brunelle, T. Jang, Optimization of poly(1,4-cyclohexylidene cyclohexane-1,4-dicarboxylate) (PCCD) preparation for increased crystallinity, Polymer 47 (2006) 4094–4104, https://doi.org/10.1016/j.polymer.2006.02.070.
[4] T.E. Sandhya, C. Ramesh, S. Sivaram, Copolyesters based on poly(butylene terephthalate)s containing cyclohexyl and cyclopentyl ring: effect of molecular structure on thermal and crystallization behavior, Macromolecules 40 (2007) 6906–6915, https://doi.org/10.1021/ma071272q.
[5] I. Bechthold, K. Bretz, S. Kabasci, R. Kopitzky, A. Springer, Succinic acid: a new platform chemical for biobased polymers from renewable resources, Chem. Eng. Technol. 31 (2008) 647–654, https://doi.org/10.1002/ceat.200800063.
[6] F. Liu, J. Zhang, J. Wang, H. Na, J. Zhu, Incorporation of 1,4-cyclohexanedicarboxylic acid into poly(butylene terephthalate)-b-poly(tetramethylene glycol) to alter thermal properties without compromising tensile and elastic properties, RSC Adv. 5 (2015) 94091–94098, https://doi.org/10.1039/C5RA18389H.
[7] F. Liu, J. Qiu, J. Wang, J. Zhang, H. Na, J. Zhu, Role of *cis*-1,4-cyclohexanedicarboxylic acid in the regulation of the structure and properties of a poly(butylene adipate-co-butylene 1,4-cyclohexanedicarboxylate) copolymer, RSC Adv. 6 (2016) 65889–65897, https://doi.org/10.1039/C6RA13495E.

[8] F. Liu, D.-Q. Chi, H.-N. Na, J. Zhu, Isothermal crystallization kinetics and crystalline morphologies of poly(butylene adipate-co-butylene 1,4-cyclohexanedicarboxylate) copolymers, Chin. J. Polym. Sci. 36 (2018) 756–764, https://doi.org/10.1007/s10118-018-2051-9.

[9] G. Guidotti, M. Soccio, V. Siracusa, M. Gazzano, A. Munari, N. Lotti, Novel random copolymers of poly(butylene 1,4-cyclohexane dicarboxylate) with outstanding barrier properties for green and sustainable packaging: content and length of aliphatic side chains as efficient tools to tailor the material's final performance, Polymers 10 (2018) 866, https://doi.org/10.3390/polym10080866.

[10] S. Singha, M.S. Hedenqvist, A review on barrier properties of poly(lactic acid)/clay nanocomposites, Polymers 12 (2020) 1095, https://doi.org/10.3390/polym12051095.

[11] S. Mohan, K. Panneerselvam, A short review on mechanical and barrier properties of polylactic acid-based films, Mater. Today Proc. 56 (2022) 3241–3246, https://doi.org/10.1016/j.matpr.2021.09.375.

[12] S. Marano, E. Laudadio, C. Minnelli, P. Stipa, Tailoring the barrier properties of PLA: a state-of-the-art review for food packaging applications, Polymers 14 (2022) 1626, https://doi.org/10.3390/polym14081626.

[13] U. Meekum, A. Khiansanoi, PLA and two components silicon rubber blends aiming for frozen foods packaging applications, Results Phys. 8 (2018) 79–88, https://doi.org/10.1016/j.rinp.2017.11.030.

[14] N. Delpouve, A. Saiter-Fourcin, S. Coiai, F. Cicogna, R. Spiniello, W. Oberhauser, S. Legnaioli, R. Ishak, E. Passaglia, Effects of organo-LDH dispersion on thermal stability, crystallinity and mechanical features of PLA, Polymer (Guildf) 208 (2020) 122952, https://doi.org/10.1016/j.polymer.2020.122952.

[15] V. Siracusa, L. Genovese, C. Ingrao, A. Munari, N. Lotti, Barrier properties of poly (propylene cyclohexanedicarboxylate) random eco-friendly copolyesters, Polymers 10 (2018) 502, https://doi.org/10.3390/polym10050502.

[16] M. Gigli, N. Lotti, M. Gazzano, V. Siracusa, L. Finelli, A. Munari, M. Dalla Rosa, Fully aliphatic copolyesters based on poly(butylene 1,4-cyclohexanedicarboxylate) with promising mechanical and barrier properties for food packaging applications, Ind. Eng. Chem. Res. 52 (2013) 12876–12886, https://doi.org/10.1021/ie401781d.

[17] G. Guidotti, G. Burzotta, M. Soccio, M. Gazzano, V. Siracusa, A. Munari, N. Lotti, Chemical modification of poly(butylene *trans*-1,4-cyclohexanedicarboxylate) by camphor: a new example of bio-based polyesters for sustainable food packaging, Polymers 13 (2021) 2707, https://doi.org/10.3390/polym13162707.

[18] G. Guidotti, L. Genovese, M. Soccio, M. Gigli, A. Munari, V. Siracusa, N. Lotti, Block copolyesters containing 2,5-furan and *trans*-1,4-cyclohexane subunits with outstanding gas barrier properties, Int. J. Mol. Sci. 20 (2019) 2187, https://doi.org/10.3390/ijms20092187.

[19] N. Bloise, E. Berardi, C. Gualandi, E. Zaghi, M. Gigli, R. Duelen, G. Ceccarelli, E. Cortesi, D. Costamagna, G. Bruni, N. Lotti, M. Focarete, L. Visai, M. Sampaolesi, Ether-oxygen containing electrospun microfibrous and sub-microfibrous scaffolds based on poly(butylene 1,4-cyclohexanedicarboxylate) for skeletal muscle tissue engineering, Int. J. Mol. Sci. 19 (2018) 3212, https://doi.org/10.3390/ijms19103212.

[20] M. Gigli, N. Lotti, M. Vercellino, L. Visai, A. Munari, Novel ether-linkages containing aliphatic copolyesters of poly(butylene 1,4-cyclohexanedicarboxylate) as promising candidates for biomedical applications, Mater. Sci. Eng. C 34 (2014) 86–97, https://doi.org/10.1016/j.msec.2013.08.013.

[21] A. Esposito, N. Delpouve, V. Causin, A. Dhotel, L. Delbreilh, E. Dargent, From a three-phase model to a continuous description of molecular mobility in semicrystalline poly(hydroxybutyrate- *co* -hydroxyvalerate), Macromolecules 49 (2016) 4850–4861, https://doi.org/10.1021/acs.macromol.6b00384.

[22] P. Pan, B. Zhu, Y. Inoue, Enthalpy relaxation and embrittlement of poly(L -lactide) during physical aging, Macromolecules 40 (2007) 9664–9671, https://doi.org/10.1021/ma071737c.

[23] M. Kwon, S.C. Lee, Y.G. Jeong, Influences of physical aging on enthalpy relaxation behavior, gas permeability, and dynamic mechanical property of polylactide films with various D-isomer contents, Macromol. Res. 18 (2010) 346–351, https://doi.org/10.1007/s13233-010-0410-7.

[24] I.N. Haugan, B. Lee, M.J. Maher, A. Zografos, H.J. Schibur, S.D. Jones, M. A. Hillmyer, F.S. Bates, Physical aging of polylactide-based graft block polymers, Macromolecules 52 (2019) 8878–8894, https://doi.org/10.1021/acs.macromol.9b01434.

[25] S. Oumnas, B. Quelennec, E. Richaud, A. Duthoit, N. Delpouve, L. Delbreilh, Post-curing and structural relaxation of epoxy networks during early stages of aging for civil engineering applications, Appl. Res. 2 (2023) e202200090, https://doi.org/10.1002/appl.202200090.

[26] A. Vashchuk, T. Missaoui, N. Delpouve, E. Dargent, Accelerated aging of 18 years rejuvenated polylactide bottles by fast scanning calorimetry, Appl. Res. 2 (2023) e202200084, https://doi.org/10.1002/appl.202200084.

[27] B. Quelennec, Z. Duan, R. Delannoy, N. Gay, M. Briffaut, V. Tognetti, N. Delpouve, L. Delbreilh, L. Bredif, A. Duthoit, E. Richaud, Effect of physical and chemical ageing on barrier properties of epoxy coating, Constr. Build. Mater. 409 (2023) 133908, https://doi.org/10.1016/j.conbuildmat.2023.133908.

[28] I. Kada, D. Trinh, S. Mallarino, S. Touzain, Physical ageing effect on water uptake and adhesion of epoxy coatings by EIS and the blister test, Electrochim. Acta 454 (2023) 142381, https://doi.org/10.1016/j.electacta.2023.142381.

[29] A.J. Kovacs, Transition vitreuse dans les polymères amorphes. Etude phénoménologique. Fortschritte Hochpolym.-Forsch, Springer-Verlag, Berlin/Heidelberg, 1964, pp. 394–507, https://doi.org/10.1007/BFb0050366.

[30] M.C. Righetti, M. Gazzano, N. Delpouve, A. Saiter, Contribution of the rigid amorphous fraction to physical ageing of semi-crystalline PLLA, Polymer 125 (2017) 241–253, https://doi.org/10.1016/j.polymer.2017.07.089.

[31] S. Xu, C. Sun, W. Yuan, J. Zhou, W. Xu, Y. Zheng, C. Yu, P. Pan, Evolution of thermal behavior, mechanical properties, and microstructure in stereocomplexable poly(lactic acid) during physical ageing, Polymer (Guildf) 249 (2022) 124840, https://doi.org/10.1016/j.polymer.2022.124840.

[32] A.T. Weyhe, E. Andersen, R. Mikkelsen, D. Yu, Accelerated physical aging of four PET copolyesters: enthalpy relaxation and yield behaviour, Polymer 278 (2023) 125987, https://doi.org/10.1016/j.polymer.2023.125987.

[33] S.G. Nunes, R. Joffe, N. Emami, P. Fernberg, S. Saseendran, A. Esposito, S. C. Amico, J. Varna, Physical aging effect on viscoelastic behavior of polymers, Compos. Part C 7 (2022) 100223, https://doi.org/10.1016/j.jcomc.2021.100223.

[34] A. Kozdras, R. Golovchak, O. Shpotyuk, S. Szymura, A. Saiter, J.-M. Saiter, Light-assisted physical aging in chalcogenide glasses: dependence on the wavelength of incident photons, J. Mater. Res. 26 (2011) 2420–2427, https://doi.org/10.1557/jmr.2011.264.

[35] R. Golovchak, J. Oelgoetz, M. Vlcek, A. Esposito, A. Saiter, J.-M. Saiter, H. Jain, Complex structural rearrangements in As-Se glasses, J. Chem. Phys. 140 (2014) 054505, https://doi.org/10.1063/1.4863561.

[36] B. Atawa, N. Couvrat, G. Coquerel, E. Dargent, A. Saiter, Chirality impact on physical ageing: an original case of a small organic molecule, Mater. Lett. 228 (2018) 141–144, https://doi.org/10.1016/j.matlet.2018.05.133.

[37] L.C.E. Struik, Physical aging in plastics and other glassy materials, Polym. Eng. Sci. 17 (1977) 165–173, https://doi.org/10.1002/pen.760170305.

[38] Y. Tanaka, H. Asano, Y. Okuya, Enthalpy relaxation near the glass transition for comb-like polymer: power law relaxation revealed by DSC experiment, J. Non-Cryst. Solids 363 (2013) 147–151, https://doi.org/10.1016/j.jnoncrysol.2012.11.050.

[39] Y. Zhang, H. Hahn, Study of the kinetics of free volume in Zr45.0Cu39.3Al7.0Ag8.7 bulk metallic glasses during isothermal relaxation by enthalpy relaxation experiments, J. Non-Cryst. Solids 355 (2009) 2616–2621, https://doi.org/10.1016/j.jnoncrysol.2009.09.003.

[40] A.J. Kovacs, J.J. Aklonis, J.M. Hutchinson, A.R. Ramos, Isobaric volume and enthalpy recovery of glasses. II. A transparent multiparameter theory, J. Polym. Sci. 17 (1979) 1097–1162, https://doi.org/10.1002/pol.1979.180170701.

[41] C.T. Moynihan, A.J. Easteal, M.A. Bolt, J. Tucker, Dependence of the fictive temperature of glass on cooling rate, J. Am. Ceram. Soc. 59 (1976) 12–16, https://doi.org/10.1111/j.1151-2916.1976.tb09376.x.

[42] J.M. Hutchinson, S. Montserrat, Y. Calventus, P. Cortés, Application of the Adam−Gibbs equation to the non-equilibrium glassy state, Macromolecules 33 (2000) 5252–5262, https://doi.org/10.1021/ma992015r.

[43] J.L. Gomez Ribelles, M. Monleon Pradas, A. Vidaurre Garayo, F. Romero Colomer, J. Mas Estelles, J.M. Meseguer Duenas, Structural relaxation of glass-forming polymers based on an equation for configurational entropy. 2. structural relaxation in polymethacrylates, Macromolecules 28 (1995) 5878–5885, https://doi.org/10.1021/ma00121a026.

[44] J. Grenet, E. Bouthegourd, A. Esposito, A. Saiter, J.M. Saiter, Is the configurational entropic model able to predict the final equilibrium state reached by Se glasses after very long ageing durations? Philos. Mag. 93 (2013) 2932–2946, https://doi.org/10.1080/14786435.2013.793482.

[45] R. Pilar, P. Honcová, G. Schulz, C. Schick, J. Málek, Enthalpy relaxation of selenium observed by fast scanning calorimetry, Thermochim. Acta 603 (2015) 142–148, https://doi.org/10.1016/j.tca.2014.09.026.

[46] Y.P. Koh, L. Grassia, S.L. Simon, Structural recovery of a single polystyrene thin film using nanocalorimetry to extend the aging time and temperature range, Thermochim. Acta 603 (2015) 135–141, https://doi.org/10.1016/j.tca.2014.08.025.

[47] X. Monnier, A. Saiter, E. Dargent, Physical aging in PLA through standard DSC and fast scanning calorimetry investigations, Thermochim. Acta 648 (2017) 13–22, https://doi.org/10.1016/j.tca.2016.12.006.

[48] D. Cangialosi, V.M. Boucher, A. Alegría, J. Colmenero, Direct evidence of two equilibration mechanisms in glassy polymers, Phys. Rev. Lett. 111 (2013) 095701, https://doi.org/10.1103/PhysRevLett.111.095701.

[49] X. Monnier, S. Marina, X. Lopez de Pariza, H. Sardón, J. Martin, D. Cangialosi, Physical aging behavior of a glassy polyether, Polymers 13 (2021) 954, https://doi.org/10.3390/polym13060954.

[50] A. Morvan, N. Delpouve, A. Vella, A. Saiter-Fourcin, Physical aging of selenium glass: assessing the double mechanism of equilibration and the crystallization process, J. Non-Cryst. Solids 570 (2021) 121013, https://doi.org/10.1016/j.jnoncrysol.2021.121013.

[51] R. Androsch, E. Zhuravlev, J.W.P. Schmelzer, C. Schick, Relaxation and crystal nucleation in polymer glasses, Eur. Polym. J. 102 (2018) 195–208, https://doi.org/10.1016/j.eurpolymj.2018.03.026.

[52] A. Morvan, L. Calvez, A. Vella, A. Saiter-Fourcin, Physical aging of the 62.5GeS2-12.5Sb2S3-25CsCl chalcogenide glass: assessing the mechanisms of equilibration and crystallization, J. Non-Cryst. Solids 598 (2022) 121955, https://doi.org/10.1016/j.jnoncrysol.2022.121955.

[53] Z. Song, C. Rodríguez-Tinoco, A. Mathew, S. Napolitano, Fast equilibration mechanisms in disordered materials mediated by slow liquid dynamics, Sci. Adv. 8 (2022) eabm7154, https://doi.org/10.1126/sciadv.abm7154.

[54] V. Mathot, M. Pyda, T. Pijpers, G. Vanden Poel, E. van de Kerkhof, S. van Herwaarden, F. van Herwaarden, A. Leenaers, The Flash DSC 1, a power compensation twin-type, chip-based fast scanning calorimeter (FSC): first findings on polymers, Thermochim. Acta 522 (2011) 36–45, https://doi.org/10.1016/j.tca.2011.02.031.

[55] J.E.K. Schawe, Measurement of the thermal glass transition of polystyrene in a cooling rate range of more than six decades, Thermochim. Acta 603 (2015) 128–134, https://doi.org/10.1016/j.tca.2014.05.025.

[56] C.T. Moynihan, A.J. Easteal, J. Wilder, J. Tucker, Dependence of the glass transition temperature on heating and cooling rate, J. Phys. Chem. 78 (1974) 2673–2677, https://doi.org/10.1021/j100619a008.
[57] M.C. Righetti, E. Mele, Structural relaxation in PLLA: contribution of different scale motions, Thermochim. Acta 672 (2019) 157–161, https://doi.org/10.1016/j.tca.2018.12.027.
[58] W.D. Cook, M. Mehrabi, G.H. Edward, Ageing and yielding in model epoxy thermosets, Polymer 40 (1999) 1209–1218, https://doi.org/10.1016/S0032-3861(98)00343-7.
[59] M.C. Righetti, G.P. Johari, Enthalpy and entropy changes during physical ageing of 20% polystyrene–80% poly(α-methylstyrene) blend and the cooling rate effects, Thermochim. Acta 607 (2015) 19–29, https://doi.org/10.1016/j.tca.2015.03.012.
[60] X. Monnier, N. Delpouve, A. Saiter-Fourcin, Distinct dynamics of structural relaxation in the amorphous phase of poly(L -lactic acid) revealed by quiescent crystallization, Soft Matter 16 (2020) 3224–3233, https://doi.org/10.1039/C9SM02541C.
[61] L. Genovese, M. Soccio, N. Lotti, A. Munari, A. Szymczyk, S. Paszkiewicz, A. Linares, A. Nogales, T.A. Ezquerra, Effect of chemical structure on the subglass relaxation dynamics of biobased polyesters as revealed by dielectric spectroscopy: 2,5-furandicarboxylic acid vs. *trans* -1,4-cyclohexanedicarboxylic acid, Phys. Chem. Chem. Phys. 20 (2018) 15696–15706, https://doi.org/10.1039/C8CP01810C.